PERGAMON

Scripta Materialia 47 (2002) 95–100

Scripta MATERIALIA

www.actamat-journals.com

Hardness and colour trends along the 76 wt.% Au (18.2 carat) line of the Au–Cu–Al system

F.C. Levey [a,1], M.B. Cortie [b,*], L.A. Cornish [c]

[a] *2600 Natta Blvd., Bellmore, NY 11710, USA*

[b] *Physical Metallurgy Division, Mintek, Private Bag X3015, Randburg 2125, South Africa*

[c] *School of Process and Materials Engineering, University of the Witwatersrand, 2050 South Africa*

Received 24 January 2002; accepted 8 April 2002

Abstract

Colour and hardness were measured on a series of alloys along the 76 wt.% Au line of the Au–Cu–Al system. Complex, non-monotonic behaviour was observed, which is shown to be correlated with microstructural changes. The available colours include reddish, yellow, 'apricot', white and purple. The hardness of as-cast material varies from 150 to 500 Vickers.

Keywords: Gold alloys; Microstructure; Hardness testing; Optical properties—absorption and transmission; Compounds—intermetallic

1. Introduction

Phase relationships in the Au–Cu–Al ternary system, particularly along the 76 wt.% Au (18.2 carat) vertical section and on the 500 °C isothermal section, have recently been determined [1,2]. During the course of those investigations, interesting trends in colour and hardness were observed. The changes along the 76% Au line are reported here, and are correlated to changes in the microstructure. The sequence investigated starts at 76% Au–24% Cu ('red gold' [3]), passes through 76% Au–19% Cu–5% Al ('Spangold' [4]) and ends at 76% Au–24% Al ('purple gold' or 'purple glory' [5]). Unless otherwise indicated, all compositions in this paper are given as wt.%.

The phase relationships, which are described elsewhere [1,2], can be summarised as follows.

The (Au,Cu) α phase extends into the ternary system from the entire Au–Cu edge. Its boundary at 500 °C and 76% Au occurs at about 1.9% Al. Next along the 76% Au line comes a ternary β phase which, on the 500 °C isothermal section, is stable between 3.0% and 5.9% Al. The binary γ-Cu_9Al_4 intermetallic compound exhibits significant solubility of Au, so much so that it extends more than half way across the ternary diagram, intersecting the 76% Au line at around 7.8% Al. The $AuAl_2$ compound exhibits a very limited solid solubility of Cu, but may be found as a single phase at Al contents of 19.6–20.6% on the 76% Au line. At 24% Al, the microstructure consists of

* Corresponding author. Tel.: +27-11-709-4475; fax: +27-11-709-4480.

E-mail address: mikec@mintek.co.za (M.B. Cortie).

[1] Formerly with Mintek, South Africa.

1359-6462/02/$ - see front matter
PII: S1359-6462(02)00100-8

$AuAl_2$+Al. Two-phase $\alpha+\beta$, $\beta+\gamma$, and $\gamma+$ $AuAl_2$ regions will also obviously be encountered along the 76% Au line between the single phase regions. The phase boundaries change for temperatures other than 500 °C—for example the β phase is formed from α by a peritectic transformation at about 750 °C [1]. However, the situation at 500 °C is broadly representative of as-cast or annealed samples, such as would be used commercially.

The properties of the 76% Au α and β phases are affected by heat treatment and thermal history. In particular, slow-cooling of the α induces an ordering transformation to the well-known AuCu-I and AuCu-II intermetallic compounds, with an attendant increase of hardness, while the β phase undergoes a reversible displacive transformation to martensite [1,4,6,7]. This latter transformation has a M_s temperature of about 29 °C and an A_s temperature of about 78 °C. The transformations in both (Au,Cu) and Spangold are accompanied by the growth of colonies of laths that are readily visible on previously polished surfaces.

2. Experimental procedure

Alloys were made using constituent elements of at least 99.9% purity. Some alloys were made by air-melting the Au in an alumina crucible in a muffle furnace, then stirring in the Cu and Al and then homogenizing the melt by stirring, remelting and stirring the alloy once more. Other alloys were arc-melted under an argon atmosphere. The compositions of the alloys were checked by analysing with EDS in a JEOL SEM at 20 kV.

Many of the initial metallographic samples were mounted in a hot mounting press, which raises their temperature to about 180 °C. When it was noticed that this caused diverse changes to the microstructures and mechanical properties of the alloys, subsequent samples were either examined unmounted, or they were mounted in cold-setting resin. There were therefore various series of samples, for example, arc-melted samples that were cold-mounted, air-melted samples that were not mounted in resin, and arc-melted samples that were annealed at 700 °C, then mounted. These are differentiated in the discussion to follow.

The hardnesses of the alloys were measured using the Vickers scale. A 5 kg load and the macroscale were used for the mounted 5 g arc-melted samples. The deformation around these hardness indentations was examined microscopically with Nomarski interference. A microhardness tester and a 1000 g load was used for the unmounted alloys.

Colour measurements were made on surfaces ground to 600 grit (p1200) using a Spectrogard colour measurement system from Pacific Scientific. The results are reported using the CIELab co-ordinate system, and were obtained after calibration with appropriate standards. This system characterises the colour of a surface by measuring its red–green component, its blue–yellow component and its white–black component, which are given as the a^*, b^* and L^* co-ordinates respectively. Each of these co-ordinates has a maximum value of $+100$ and a minimum value of -100, with white being $L^*=+100$, black being $L^*=-100$, red occurring at $a^*=+100$, green at $a^*=-100$, yellow at $b^*=+100$ and blue at $b^*=-100$. Attempts have been made to use this system to standardise colour measurements in the jewellery industry [8]. Since the variation in L^* values for the present metallic samples was not large, the results have been plotted here as b^* *vs* a^* for clarity. The colour measurements of the alloys under investigation are also compared with published colour measurements of standard jewellery alloys [8–10].

3. Results

3.1. Hardness measurements and related effects

The variation in hardness with Al content across the 76% Au vertical section is shown in Fig. 1. The trend in hardness values of all the alloys was consistent at compositions above 6% Al. At compositions up to 6% Al, the macro-hardness values of the annealed and mounted alloys, shown by the dashed line, closely followed the trend of the micro-hardness values of the unmounted air-melted alloys. However, these two sets of values

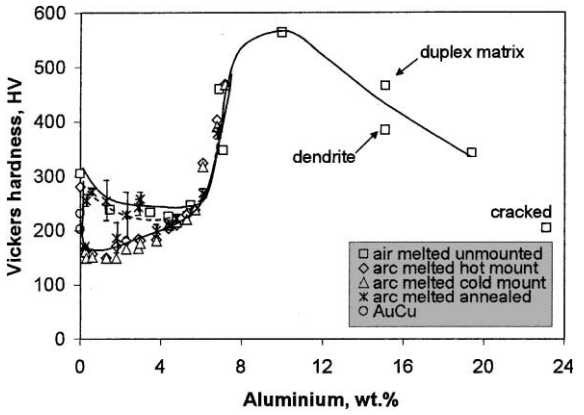

Fig. 1. Change in hardness on progressing along 76 wt.% Au line in Au–Cu–Al system.

were higher than the macro-hardness values for the corresponding samples that had been arc-melted but not annealed prior to mounting. There are two possible explanations for the observed disparity in hardness measurements. The first is that the mounting processes caused some softening in the as-cast alloys. The second is that the oxidation produced by the annealing process caused varying degrees of oxidation of the grain boundaries, thereby increasing the hardnesses of the annealed arc-melted alloys, and causing the large scatter in the measurements. The higher hardnesses of the air-melted alloys could be attributed to the formation of a relatively large elastic deformation compared with plastic deformation during micro-hardness testing, with a resultant decrease in the apparent size of the indentation and a higher hardness reading. This phenomenon has been observed by others in shape memory alloys at temperatures a little below A_f [11].

The Au–24% Cu–0% Al samples, which had the 1:1 stoichiometry of the AuCu-I phase, were relatively hard, but the hardness decreased rapidly on addition of Al. X-ray diffraction indicated that the Au–24% Cu samples were in fact partially ordered [12], which explained their relatively high hardness. However, even very small additions of Al evidently either retard the ordering kinetics of AuCu or depress its ordering temperature, or perhaps even induce solid solution softening, as is reportedly the case in Cu_3Au [13].

There was a systematic increase in hardness in the un-annealed arc-melted samples containing between 1.9% and 5.7% Al, from about 150 HV to more than 210 HV, indicating that the β phase of these alloys was hardened by Al in solid solution. This increase in hardness was not observed in the unmounted air-melted alloys or the annealed and mounted arc-melted alloys.

Between 5.7% and 7.2% Al, there was a sharp increase in hardness due to the increasing presence of γ-Cu_9Al_4. With further Al additions, the hardness increased further to a maximum of about 500 HV at 10% Al. The microstructure of this sample consisted of a dendrites of γ-Cu_9Al_4 with $AuAl_2$ at the grain boundaries, apparently formed by a divorced eutectic reaction [14]. At higher Al contents, the microstructure changed to dendrites of $AuAl_2$ in a duplex matrix of γ-$Cu_9Al_4 + AuAl_2$. The hardnesses of both the $AuAl_2$ dendrites and the interdendritic matrix were measured for the 15.0% Al alloy, and are shown in Fig. 1. It is interesting to note that the $AuAl_2$ dendrites were softer than the surrounding two-phase matrix, which indicates that the ternary extension of γ-Cu_9Al_4 is harder than the $AuAl_2$ phase. However, the $AuAl_2$ dendrites in the 15.0% Al sample were significantly harder than those of the 19.4% Al alloy. This is possibly due to solid solution hardening by the additional Cu in the dendrites of the 15.0% Al alloy. The hardness of the 23.1% Al sample was low. Further metallographic inspection revealed that the alloy had cracked at the corners of the indentations under the applied load. This is typical of single-phase $AuAl_2$ samples, which are relatively soft but brittle, with a typical hardness of about 200–250 HV, depending on stoichiometry and method of preparation.

3.2. Stress-induced martensite and twinning

Surface deformation occurred around the macro-hardness indentations on samples that contained α or β phase. The type of deformation was consistent with the observed general microstructures of the alloys. There was twinning around the indentations of the 0–1.8% Al α-phase alloys (Fig. 2), which appeared as parallel lines radiating from the hardness indentations. A mixture of

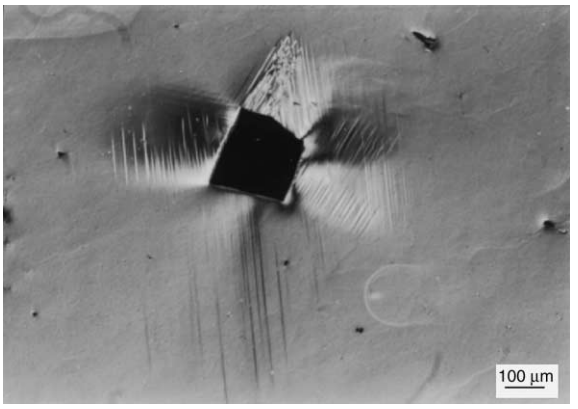

Fig. 2. Twinning induced around the site of a macro-hardness indentation in an α-phase sample.

stress-induced martensite (SIM) and twinning surrounded the indentations of the $\alpha + \beta$ phase alloys, and well-defined colonies of SIM laths formed around indentations in the 3.8–5.8% Al β-phase alloys (Fig. 3). The morphology of observed SIM was considerably different to that of the twins, and consisted of wedge-shaped laths with noticeable height differences when viewed with Nomarsky interference. A two-phase structure was evident in the 6.1–7.2% Al alloys, together with sporadic patches of laths in any sufficiently large regions of β phase in the vicinity of the induced stress.

No stress-induced deformation was evident around the micro-hardness indentations. Evidently, if any SIM was formed in these instances, it reverted to parent phase when the indentor was removed. As mentioned earlier, the presence of stress-induced deformation around the macro-hardness indentations could have been due to the macro-hardness indentations being accompanied by a larger volume of irreversible plastic deformation than the micro-hardness indentations.

3.3. Colour measurements

The trends in a^* and b^* values with increasing Al contents are shown in Fig. 4. The redness, or a^*, values of the cold mounted samples were reduced by three points since the mounting resin was pink, and the light spot used for the measurements covered both the small sample and approximately an equal quantity of the surrounding resin. Some known metals and standard red, yellow and green jewellery alloys, also with a 600 grit surface finish, are shown on the graph for reference.

The colour trends of all four sets of alloys were similar. As expected, the addition of Al–AuCu initially bleached the red component of the alloys (point *a* on Fig. 4), so that they became progressively lighter and more yellow as opposed to the rich red–gold colour of the 0% Al alloy. At around 3% Al, the edge of the β phase field, the alloys had a lemon-yellow colour (point *b*), similar to that of the standard commercial 2N18Y alloy [8].

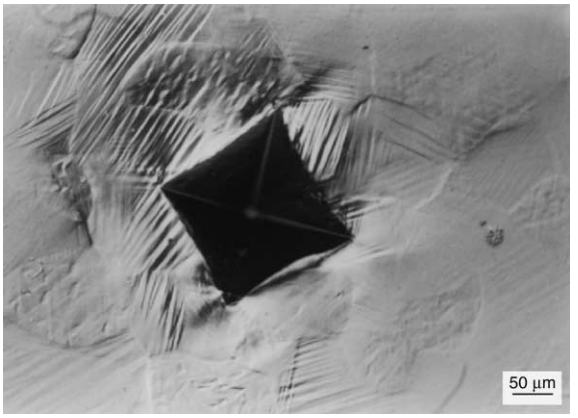

Fig. 3. Laths of stress-induced martensite around a macro-hardness indentation in a β-phase sample.

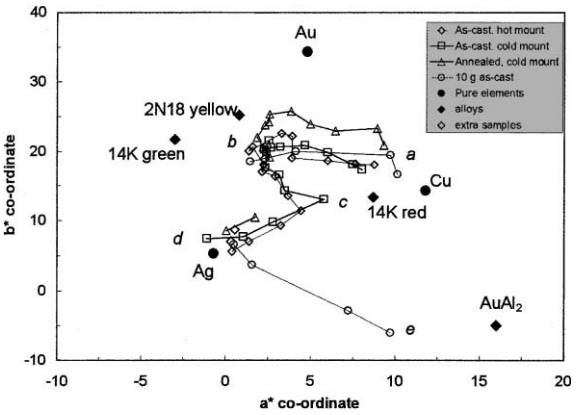

Fig. 4. Colour variation across the76 wt.% Au vertical section; *a*—0% Al, *b*—3% Al, *c*—5.8% Al, *d*—7.2% Al, *e*—24% Al.

Contrary to expectation, as the Al content of the alloys was increased across the β phase field, both the red and blue components increased, so that the alloys became progressively more pink. The nominally 6% Al alloys had a characteristic and unusual pinkish hue christened 'apricot' (point *c* on Fig. 2), and which is reminiscent of the standard 14 K red composition [8]. The variation across the β phase is possibly due to the same phenomenon described by Saeger and Rodies [15], where a change in the electronic structure of the intermetallic compound can occur with varying composition, causing a different portion of the visible spectrum to be reflected from the surface of the alloy. From 6.1% to 7.2% Al, the colour was bleached once again, apparently due to the presence of the γ-Cu_9Al_4 phase, so that the 7.2% Al as-cast arc-melted alloy was almost as white as pure silver (point *d*). With further increases in the Al content, the colour reflected from the surfaces of the alloys changed progressively from white through to a deep pink-purple (point *e*) as the volume fraction of $AuAl_2$ increased, although not quite reaching the intensity of the pure $AuAl_2$ compound.

4. Discussion

Colour and hardness are two important characteristics of jewellery alloys. In an ideal world, one would have a wear-resistant, ductile alloy with a striking colour and an interesting surface texture. However, wear resistance is in general related to an increased hardness, which in turn often causes a decrease in the ductility and therefore workability and toughness of the alloy.

Since a potential application of the Spangold alloys is in jewellery, it is useful to have characterised the colour and hardness trends in these and other alloys in the Al–Au–Cu system. The nominally 6% Al alloy has a striking colour, but is more brittle than its 5% Al counterpart, which has a colour very similar to well-known commercial jewellery alloys. A compromise can be reached by making an alloy with 5.5% Al, which has a more subtle pink hue than the 6% Al alloy, but has somewhat improved mechanical properties.

Another potential application for these alloys would be in shape memory systems, since the 6% Al alloy has exhibited some characteristics associated with shape memory alloys [6]. In this case, colour would not be important, and the ductility and oxidation resistance of the grain boundaries would be a greater design consideration. The lack of mechanical strength of the 6% Al alloy is thought to be related to the presence of a thin intergranular film of the γ-Cu_9Al_4 intermetallic compound. Therefore, an alloy with a composition closer to the $\alpha + \beta$ boundary, and also with either more or less Au may be found to be more ductile, while still exhibiting shape memory properties and a similar hardness.

The 7.5% Al alloy has a colour that is very similar to that of silver, and could certainly be regarded as an example of an 18 carat, nickel-free, white gold composition. Unfortunately, its great hardness and poor ductility would greatly restrict its commercial application. Finally, the 24% Al alloy, with its striking purple colour, may have jewellery applications due to the presence of Al at the grain boundaries, which may give the alloy more structural integrity than the pure form of $AuAl_2$.

5. Conclusions

1. A number of Au–Cu–Al alloys were produced along the 76 wt.% Au section (theoretically from $Au_{50.5}Cu_{49.5}$ to $Au_{30.25}Al_{69.75}$). The hardness and colour trends of these alloys were measured to characterise material properties in this system.
2. The addition of Al to the α phase of 'red gold' softens the alloy and reduces the intensity of its red colour component. These trends reach their minima at about 3% Al, which corresponds with the start of β phase field and a 'lemon-yellow' colour.
3. Increasing the Al content of the β phase from 3% to 5.8% causes it to increase in hardness from about 150 to 200 HV, and also to systematically acquire an orange–pink hue, designated as 'apricot'.
4. Cu_9Al_4, a hard, brittle intermetallic phase with the γ-brass structure, cuts the 76% Au line at

about 7.8% Al. It is silver–white in colour, and its presence rapidly bleaches the 'apricot' hue of the edge of the β phase.

5. The relatively soft $AuAl_2$ phase appears at Al contents greater than 8.1%. It is bright purple in colour, and causes the colour of the 76% Au alloys with between 8.1% and 24% Al to vary from white through mauve to purple.
6. The hardness of the two-phase γ-Cu_9Al_4 + $AuAl_2$ alloys is very sensitive to their proportions within the microstructures, because the $AuAl_2$ phase has a hardness of only about 200 HV while that of the Cu_9Al_4 phase is about 500 HV.
7. The microstructures of the 0%–7.2% alloys came out in relief around the hardness indentations due to the occurrence of stress-induced twinning in α phase and stress-induced martensite in β phase.

References

[1] Levey FC. Phase relationships, transformation behaviour and material properties in Au–Cu–Al, PhD thesis. Johannesburg: University of the Witwatersrand; 2000.
[2] Levey FC, Cortie MB, Biggs T, Ellis P. Proc Microsc Soc Southern Africa 1998;28:18.
[3] McDonald AS, Sistare GH. Gold Bull 1978;11:66.
[4] Cortie M, Wolff I, Levey F, Taylor S, Watt R, Pretorius R. Gold Technol 1994;14:30.
[5] Cahn RW. Nature 1998;396:523.
[6] Levey FC, Cortie MB, Cornish LA. Metall Mater Trans A 2000;31:1917.
[7] Levey FC, Cortie MB. Mat Sci Eng 2001;A303:1.
[8] Cretu C, Van der Lingen E. Gold Bull 1999;32:115.
[9] Raykhtsaum G, Agarwal DP. Am Jewelry Manufact 1991:18.
[10] Roberts EFI, Clarke KM. Gold Bull 1979;12:9.
[11] Hornbogen E, Kobus E. Prakt Metallog 1993;30:507.
[12] Cortie MB, Levey FC. Intermetallics 2000;8:793–804.
[13] Chapman MR, Gillam E. Scripta Metall 1970;4:145.
[14] Chadwick GA. In: Metallography of phase transformations. London: Butterworths; 1972. p. 145.
[15] Saeger KE, Rodies J. Gold Bull 1977;10:10.